Role of boundary conditions in an experimental model of epithelial wound healing

Djordje L. Nikolic, Alistair N. Boettiger, Dafna Bar-Sagi, Jeffrey D. Carbeck and Stanislav Y. Shvartsman

Am J Physiol Cell Physiol 291:68-75, 2006. First published Feb 22, 2006;
doi:10.1152/ajpcell.00411.2005

Am J Physiol Cell Physiol 291: C68–C75, 2006.
First published February 22, 2006; doi:10.1152/ajpcell.00411.2005.

Role of boundary conditions in an experimental model of epithelial wound healing

Djordje L. Nikolić,[1] Alistair N. Boettiger,[2] Dafna Bar-Sagi,[3] Jeffrey D. Carbeck,[1] and Stanislav Y. Shvartsman[1,4]

[1]*Department of Chemical Engineering and* [2]*Department of Physics, Princeton University, Princeton;* [3]*Department of Molecular Genetics and Microbiology, State University of New York Stony Brook, Stony Brook, New York; and* [4]*Lewis-Sigler Institute for Integrative Genomics, Princeton University, Princeton, New Jersey*

Submitted 12 August 2005; accepted in final form 19 February 2006

Nikolić, Djordje L., Alistair N. Boettiger, Dafna Bar-Sagi, Jeffrey D. Carbeck, and Stanislav Y. Shvartsman. Role of boundary conditions in an experimental model of epithelial wound healing. *Am J Physiol Cell Physiol* 291: C68–C75, 2006. First published February 22, 2006; doi:10.1152/ajpcell.00411.2005.—Coordinated cell movements in epithelial layers are essential for proper tissue morphogenesis and homeostasis, but our understanding of the mechanisms that coordinate the behavior of multiple cells in these processes is far from complete. Recent experiments with Madin-Darby canine kidney epithelial monolayers revealed a wave-like pattern of injury-induced MAPK activation and showed that it is essential for collective cell migration after wounding. To investigate the effects of the different aspects of wounding on cell sheet migration, we engineered a system that allowed us to dissect the classic wound healing assay. We studied Madin-Darby canine kidney sheet migration under three different conditions: *1*) the classic wound healing assay, *2*) empty space induction, where a confluent monolayer is grown adjacent to a slab of polydimethylsiloxane and the monolayer is not injured but allowed to migrate upon removal of the slab, and *3*) injury via polydimethylsiloxane membrane peel-off, where an injured monolayer migrates onto plain tissue culture surface, as in the case of empty space induction allowing for direct comparison. By tracking the motion of individual cells within the sheet under these three conditions, we show how the dynamics of the individual cells' motion is responsible for the coordinated migration of the sheet and is coordinated with the activation of ERK1/2 MAPK. In addition, we demonstrate that the propagation of the waves of MAPK activation depends on the generation of reactive oxygen species at the wound edge.

ERK; reactive oxygen species; coordinated cell sheet migration; cell communication; multicellular dynamics; surface patterning

COORDINATED CELL MOVEMENTS in epithelial layers are essential for proper tissue morphogenesis and homeostasis (17). Folding of epithelial sheets during gastrulation and appendage morphogenesis, and cell sheet migration during wound healing are just a few from a long list of examples. Our understanding of the mechanisms that coordinate the behavior of multiple cells in these processes is far from complete. The main goal is to understand how multiple cells execute highly dynamic and coordinated movements, while preserving the integrity of the epithelium. Recent experiments (4) in embryonic development reveal that epithelial sheet dynamics can be regulated by the spatiotemporal patterns of the activation of ERK1/2 MAPK, a highly conserved signal transduction module. For example, periodic pulses of MAPK activation control delamination of small clusters of cells from the *Drosophila* embryonic ectoderm (3). In mouse development, MAPK driven by locally produced growth factors orchestrates cell shape changes during the eyelid closure (19, 27).

In embryogenesis, a significant fraction of the cell-cell coordination in epithelial sheet dynamics may be derived from the spatial patterns of gene expression imposed at earlier stages of development (16). In wound healing, the location of cells with respect to the wound can provide positional information for their collective behavior during tissue repair (9, 16). Experiments with epithelial monolayers of Madin-Darby canine kidney (MDCK) cells showed that wounding in this model system is accompanied by two traveling waves of MAPK activation that propagate from the wound edge into the bulk of the monolayer (18). These dynamic signaling patterns were found to be essential for coordinated cell migration during wound healing, which involves spreading of the monolayer, with essentially no cell division. Furthermore, it has been proposed that MAPK participates in a positive feedback loop (Fig. 1*A*) composed of cell spreading, MAPK activation, and cell migration, which drives the spreading of a wounded MDCK monolayer (18).

Wounding of an intact epithelium both injures the cells and provides free space, enabling cell spreading and sheet migration. If MAPK indeed forms a part of a positive feedback loop, then unconstraining of the epithelial monolayer may be sufficient to initiate self-sustained sheet migration even in the absence of injury. Such a hypothesis has been recently proposed on the basis of experiments with corneal epithelium monolayers (2). In this study, we test this hypothesis in wounded MDCK monolayers, a system with rich MAPK dynamics with an established role in sheet spreading (18), using a combination of cell tracking experiments and surface patterning techniques.

By manipulating the initial and boundary conditions of an MDCK monolayer, we show that an injury is essential for coordinated behavior of cells in the epithelial sheet in this system. We find that the first wave of MAPK activation is induced by injury and that unconstraining of the sheet without injury induces only the second, slower wave of MAPK activation. We show that, immediately following injury, reactive oxygen species (ROS) are generated at the wound interface, and demonstrate that ROS are essential for the generation of

Address for reprint requests and other correspondence: S. Y. Shvartsman, Lewis-Sigler Institute for Integrative Genomics, Carl Icahn Laboratory, Washington Rd., Princeton University, Princeton, NJ 08544 (e-mail: stas@princeton.edu).

The costs of publication of this article were defrayed in part by the payment of page charges. The article must therefore be hereby marked "*advertisement*" in accordance with 18 U.S.C. Section 1734 solely to indicate this fact.

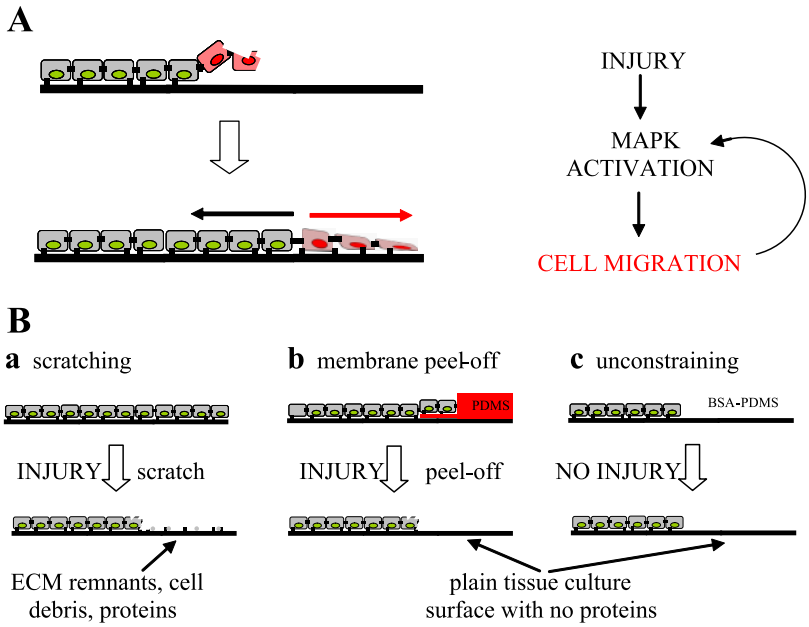

Fig. 1. *A*: feedback loop between the epithelial cell migration and MAPK ERK 1/2 activation, based on the study by Matsubayashi et al. (18). *B*: comparison of the three "boundary conditions" used in the wounding experiments. *a*, Scraping the cells off with a pipette generates a wound, where the injured cell sheet moves on remnants of extracellular matrix (ECM), cell debris, and other adsorbed proteins. *b*, Ripping off a polydimethylsiloxane (PDMS) membrane generates a wound, where an injured cell sheet migrates over plain tissue culture surface. *c*, Removal of a BSA-blocked PDMS slab unconstrains the sheet, where an uninjured cell sheet migrates over the plain tissue culture surface.

the first (fast) wave of MAPK activation that spreads through the layer. We present the results of cell tracking analysis in the spreading MDCK epithelium and discuss the correlation between MAPK signaling and the dynamics of cell sheet migration. While the origin of the MAPK waves in MDCK epithelial wound healing remains to be elucidated by further experiments, our analysis should enable the formulation of increasingly quantitative models of epithelial sheet dynamics in wound healing and embryogenesis.

MATERIALS AND METHODS

Cell culture. MDCK cells (purchased from ATCC, Manassas, VA) were maintained in Dulbecco's modified Eagle's medium (Invitrogen, Carlsbad, CA) supplemented with 10% fetal bovine serum (Sigma, St. Louis, MO), 10 mM HEPES buffer, pH 7.4 (Invitrogen), and antibiotics (50 U/ml penicillin and 50 μg/ml streptomycin, Sigma) at 37°C, 5% CO_2 and 80–90% humidity in an incubator.

Wound closure and cell tracking. MDCK cells were plated in a tissue culture 24-well plate at an initial density of 1.5×10^5 cells/cm^2. A uniform monolayer formed in ~2–3 days. All wounding assays were performed in a serum-free medium by first preincubating the cells in the serum-free medium for 30 min before the start of the experiments. A micropipette was used to create a wound in the monolayer by scraping. Wound closure was followed for 16 h by phase-contrast microscopy on a Zeiss Axiovert 200M microscope and digital images of the wound area were taken once every 5 min with a Hamamatsu Orka-ER charge-coupled device (CCD) camera. Image analysis and cell tracking were done manually, by selecting individual cells with IPLab software (Scanalytics, Fairfax, VA) and extracting the centroid position of a cell.

Immunofluorescence. Cells were fixed with freshly prepared 4% formaldehyde solution (Sigma). After permeabilizing with 5% Triton X-100 (Sigma) in PBS, and blocking with 10% horse serum (Sigma) in 3% BSA (Sigma) in PBS, cells were incubated in rabbit antiphosphoERK1/2 antibody (Cell Signaling Technologies, Beverly, MA) overnight at 4°C, followed by 1 h incubation with anti-rabbit Alexa 568 secondary antibody (Molecular Probes, Portland, OR). The primary antibody (concentration of 0.2 mg/ml) was diluted at 50:1 and the secondary (concentration of 2 mg/ml) at 400:1, both in 3% BSA solution in PBS (Invitrogen). The surfaces were mounted with antifading Fluoroguard (Bio-Rad Laboratories, Hercules, CA) and digital pictures were taken on an inverted Nikon Eclipse TE300 microscope with a Photometrics CoolSnap FX CCD camera (Roper Scientific, Tucson, AZ). The images were analyzed with IPLab software. For the analysis of the spatiotemporal patterns of MAPK activation, 10 lines were drawn across each image at random and the fluorescence intensity across each of the lines averaged. The average intensity across these 10 slices was then examined and a noticeable drop-off in the intensity of fluorescence was taken as an indication of the ending point the signal reached. The intensity plots shown are the normalized values of intensity to the maximal signal in each image. All optical and camera settings were kept constant throughout image acquisition.

Inhibition of ERK1/2. To inhibit MAPK ERK1/2, UO126 (Promega, Madison, WI) was added to the culture at the concentration of 20 μg/ml (as described in Ref. 18) in anhydrous DMSO (Sigma) at the same time when serum was removed.

Manipulation of boundary conditions for model wounds. Slabs of polydimethylsiloxane (PDMS; Dow Corning, Midland, MI) were created by modifying a previously published procedure for cell patterning with polymeric membranes (12, 21). Briefly, PDMS was mixed at 10:1 precursor/curer ratio, poured over a silicon wafer in a petri dish to ~7 mm height, degassed in a desiccator for at least 1 h, and baked for at least 2 h in a 65°C. Blocks of PDMS roughly 5 mm × 5 mm (already 7 mm high) were cut with a razor, extracted in dichloromethane (Sigma) for 24 h, dried overnight, sterilized with ethanol and then blocked in 3% heat denatured BSA in PBS for 1 h. The slabs were then placed onto a tissue culture surface allowing for a conformal contact with the surface and seeded with MDCK cells at the same density as when no PDMS was present. The hydrophobic to hydrophobic interactions between the PDMS slab and the tissue culture surface resulting from the conformal contact (complete contact between surfaces) prevented the contact of medium and cells with the tissue culture surface under the PDMS slab (21). Once a uniform epithelial monolayer formed, the slab was lifted with sterile tweezers to create an empty space next to a noninjured uniform epithelial monolayer, effectively unconstraining the cells. PDMS membranes (very thin, ~30 μm, layers of PDMS) were created as published previously (12, 21). Briefly, PDMS was mixed as stated above and then dissolved in a 1:1 wt:wt ratio in toluene (Sigma). One milliliter of 1,1,1,3,3,3-hexamethyldisilazane (Sigma) was spin coated (a process that uses the centripetal force to coat a spinning surface) onto a

2-in. silicon wafer (Universitywafer.com, South Boston, MA) at 3,000 rpm for 40 s, and then about a quarter coin size of POMS-toluene solution was poured onto the wafer and spin-coated at 900 rpm for 60 s. For easier handling of the membranes, the edges were built up with an addition of another PDMS layer. The membranes were then baked for at least 2 h in a 65°C oven. Additional layers of PDMS on the edges could be added once the previous layer had solidified. The membranes were cut with a razor, peeled off, extracted in dichloromethane for 24 h, dried overnight, sterilized with ethanol, and then placed on a tissue culture surface allowing for a conformal contact with the surface and seeded with MDCK cells. Once a uniform monolayer was formed, the membrane was peeled off with sterile tweezers ripping the epithelial sheet that had partly grown over it, forming an injured monolayer next to the plain tissue culture surface.

Data analysis. At least 45 cells were tracked for each of the 4 treatments. The displacement of a cell was calculated as the Euclidean distance between the $n + 1$ and n positions in time. Total displacement was calculated as the Euclidean distance between n_{final} and $n_{initial}$ positions of a cell. The correlation coefficient was calculated in MATLAB (Mathworks, Natick, MA) using the corrcoef.m function. Confidence intervals for correlation coefficients were computed with the use of the Bootstrap method (25). All experiments were replicated at least three times, and the data presented here are from a representative experiment.

Visualization and inhibition of ROS. The dye solution 5-(and-6)-chloromethyl-2′,7′-dichlorodihydrofluorescein diacetate, acetyl ester (CM-H_2DCFDA; Invitrogen) was used to visualize the formation of ROS. The dye was first diluted to a stock solution of 1,000 μM in anhydrous DMSO immediately before use. Phenol red-free DMEM (Invitrogen) was used as a loading solution, into which the dye was diluted to a working concentration of 5 μM immediately before use. The working concentration was empirically obtained from the suggested guidelines from the manufacturer. The cells were incubated in this loading solution for 30 min before wounding the monolayer. The fluorescent signal used to detect the ROS results from the intracellular removal of the acetate groups of CM-H_2DCFDA. Because the fluorescent species is removed relatively quickly from cells by an active efflux (as stated by the manufacturer), we implemented extensive controls to obtain the correct duration of the ROS wave presence in the cells. CM-H_2DCFDA was added at different times after the injury. This allowed us to test for the presence of ROS at different times (from minutes to hours) after the injury. The digital pictures were taken on an inverted Nikon Eclipse TE300 microscope with a Photometrics CoolSnap FX CCD camera. The images were analyzed with IPLab software. To inhibit the formation of ROS, *N*-acetyl-L-cysteine (Sigma) was added to the culture at the same time when the serum was removed at a concentration of 5 μM (29).

RESULTS

Analysis of waves of MAPK activation after mechanical injury. In agreement with the results of Matsubayashi et al., we observed two waves of ERK1/2 MAPK phosphorylation after mechanical wounding of the MDCK epithelial monolayer (Fig. 2). At the level of individual cells, the first wave was transient and peaked at ~3 min after wounding. This wave reached ~500 μm into the cell sheet from the wound interface (Fig. 3); it was receding by ~5 min after wounding and was confined only to the first row of cells at the wound interface by ~10 min after wounding. After ~30 min, the second wave of MAPK phosphorylation initiated close to the wound boundary; by 4 h after wounding, this wave propagated ~500 μm into the cell sheet (Fig. 3). At the level of individual cells, the second wave led to sustained MAPK phosphorylation (measurement were stopped after 18 h, results not shown).

In a wounding experiment, MAPK activation can be induced by a combination of the injury itself and the processes enabled by the availability of the empty space (cell migration, new interactions with the substrate, etc.). Recent experiments in corneal epithelial wound healing led to the hypothesis that MAPK activation can be induced as a result of unconstraining the cells in the epithelial layer, thus enabling their migration (2). To separate the effects of mechanical injury from those induced by the sudden availability of empty space, we devised a method that allowed us to induce empty space in an epithelial sheet with minimal physical disturbance to the monolayer and no cell damage.

A nonadhesive elastomeric PDMS slab was placed on a tissue culture surface where cells were subsequently seeded. After a monolayer was formed, the slab was lifted, not damaging the cells but removing a physical barrier for sheet migration (12, 21). When the MDCK monolayer was unconstrained in this manner, the spatiotemporal pattern of MAPK phosphorylation was different from the one seen in a wounding assay: only one wave of signal propagation was observed. This wave coincided with the second wave observed after scratching, both temporally and spatially, reaching ~500 μm 4 h after unconstraining (Fig. 3). This experiment allowed us to dissect the two waves of MAPK phosphorylation observed in the classical wounding experiment and demonstrate that only the slow wave of MAPK activation is induced in the absence of injury.

In these two cases, however, the surfaces on which the epithelial sheet was migrating were different (Fig. 1*B*). In the case of an injury created by scratching, cells were scraped off the tissue culture surface, leaving behind the remnants of cell-deposited extracellular matrix, cell debris, and other proteins that might have adsorbed from serum during the time that the cell sheet was grown to confluency. On the other hand, when empty space was induced into a monolayer via removal of a PDMS slab, the surface underlying the slab had not come into contact with any proteins or cell debris, thus presenting the monolayer with a plain tissue culture surface onto which to migrate. The presence of the proteins in the first case and their absence in the second was verified by immunofluorescence staining for fibronectin (results not shown), a major extracellular matrix protein that is also present in the serum, and ELISA for fibronectin as well (results not shown). In the latter case, PDMS interacts with the tissue culture surface via hydrophobic forces, acting as a cover that prevents proteins from adsorbing onto the surface, maintaining it denuded. The presence of fibronectin on the surface after the scraping of the cells and its absence in the case of PDMS slab removal are a clear indication of the distinct differences between the surfaces in these two treatments. We have observed reproducible reduction of fibronectin levels in PDMS-covered wells; furthermore, the extent of reduction correlated with the fractional area of the surface covered with PDMS (results not shown).

The type, quantity, and the spatial distribution of adhesive ligands on the surface can greatly affect cell migration (15). We therefore wanted to devise a method that would allow us to study just the effects of initial mechanical injury, with the cell monolayers migrating on the same kind of surface. The peeling off of a PDMS membrane over which a monolayer had partially grown (Fig. 1*B*) allowed us to do that. In this case, as in the case of a "scratch" assay, the two waves of MAPK

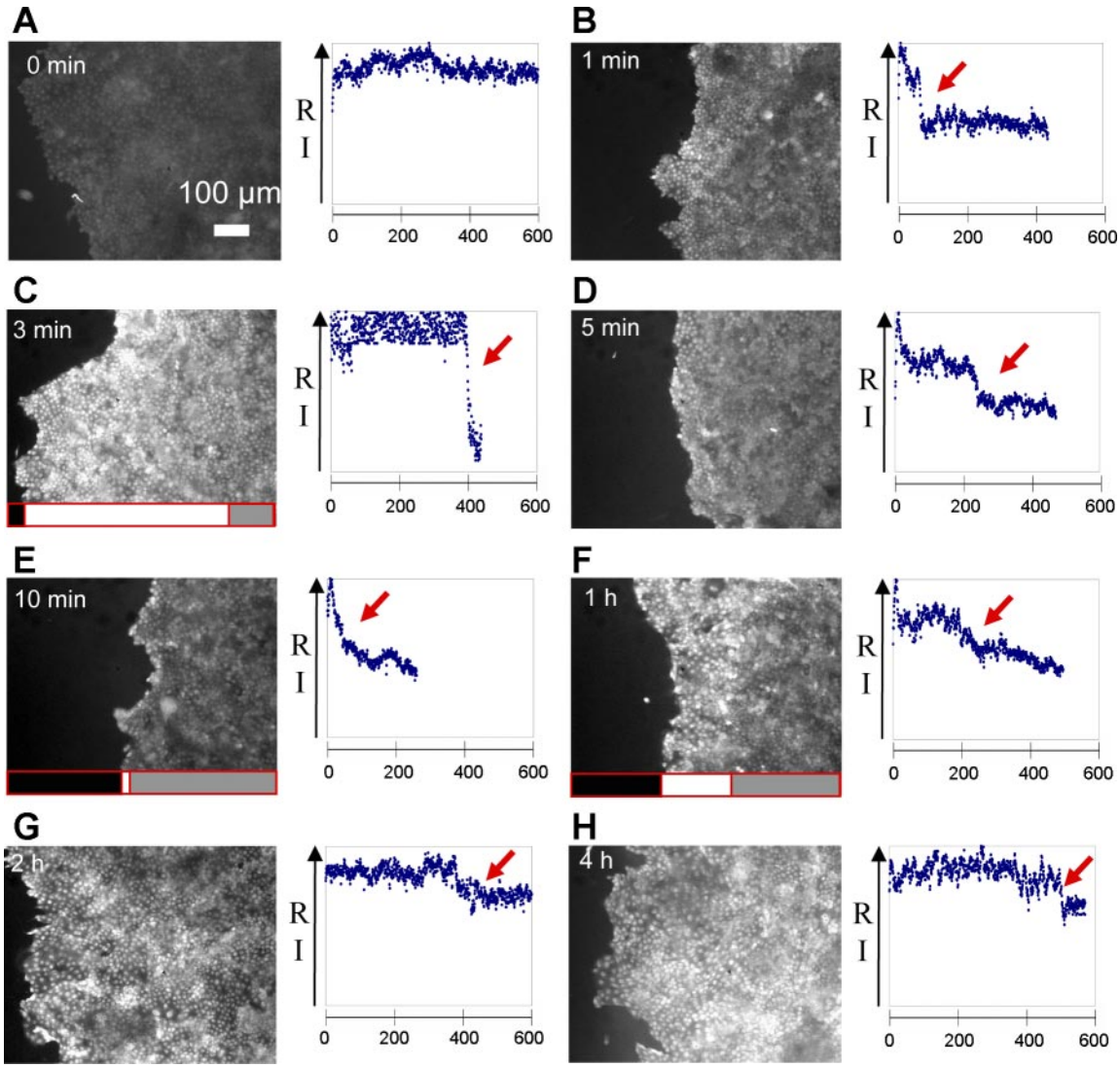

Fig. 2. Waves of MAPK activation observed after wounding: a transient wave on the time scale of minutes and a sustained wave on the time scale of hours. *Left*: immunofluorescence images of phosphorylated ERK1/2 in the epithelial sheet wounded by scratching (*A–H*). *Right*: fluorescence intensity averaged in the direction normal to the wound. The arrow marks the location of the wave front (associated with the drop-off in the averaged intensity, see text for more details). *Inset*, scales at the bottom of images *C*, *E*, and *F*, where white represents the presence and gray the absence of the signal, pictorially represent the distance the MAPK wave reached in that particular case. RI, relative intensity.

activation were observed, with similar characteristics to the MAPK waves observed after a scratch (Fig. 3), suggesting a similar kind of signaling response to these two kinds of injury. On the basis of these experiments, we conclude that the primary wave of MAPK phosphorylation is induced by injury alone. Finally, the coincidence of the secondary MAPK phosphorylation waves in all three experimental designs (injury, PDMS slab removal, and membrane peel-off) suggests that the two phases of MAPK phosphorylation can be decoupled.

Displacement of individual cells in a spreading epithelial sheet. To gain further insight into the epithelial sheet dynamics after wounding, we followed cell migration by video time-lapse microscopy. Images were taken every 5 min, a time interval small enough for a detailed tracking analysis of a cell's path. Figure 4 shows positions of 45 cells in the epithelial sheet wounded by scratching. We found that cells in the epithelial sheet move in a highly coordinated manner: at any given moment in time, the distance traveled by the cell correlates with the initial distance of the cell from the wound. For example, Fig. 5*A* shows the distances traveled by individual cells at different times, as a function of the initial distance of the cell from the wound interface. Figure 6*A* shows the correlation between the total displacements of cells (>16 h after wounding) with their initial coordinates. These measurements suggest that, following wounding, the epithelial sheet moves in a quasi one-dimensional way, like a rubber band "pulled" into the denuded area. This is clearly supported by Fig. 7*A*, which shows the coordinates of a group of cells aligned normal to the wound interface.

It has been suggested that the availability of empty space is sufficient to initiate coordinated migration of an epithelial sheet, similar to the one observed in wound healing experiments (2). To test this hypothesis, we followed cell migration in a monolayer after PDMS unconstraining (see above). Over-

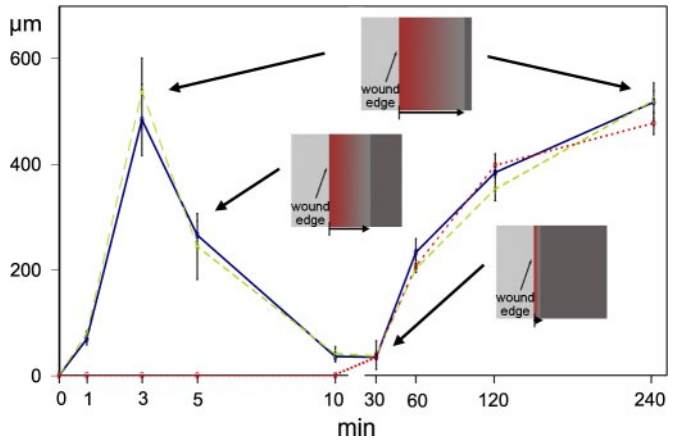

Fig. 3. Distance from the wound edge that MAPK wave reaches at different time points after wounding. In both cases of injuring: scratching (solid trace) or membrane peel-off (dashed trace), both waves are present with similar characteristics. In the case of unconstraining without injuring (dotted trace), only one wave is present. The values represent an average of 3 experiments with 1 standard deviation presented by error bars. *Insets*, schematic representation of the MAPK waves reaching different distances at different times.

all, the migratory behavior of the sheet and of individual cells was greatly attenuated compared with the scratch-wounded monolayer (compare Fig. 5, *A* and *C*). The cells migrated with slower speeds and their paths were less persistent (data not shown). In addition, distances traveled by cells in this case exhibited essentially no correlation with their position in the monolayer (Fig. 6*C*). Thus, the behavior was very different from the one of the scratch-wounded layer, where cells moved in a highly coordinated manner. On the basis of these experiments we conclude that the secondary (slow) wave of ERK1/2 MAPK phosphorylation alone is not sufficient to induce the migration of an MDCK epithelial sheet. This difference can be due to the differences in the surface that the cells have to migrate on and/or the absence of injury.

To dissect the effects of surface properties and cell injury on the overall sheet migration, we followed migration of individual cells in the membrane peel-off experiments, a treatment in which the cells are injured, but migrate on a plain tissue culture surface. If the injury alone is sufficient to initiate the coordinated migration of cells in the epithelial layer, then we should expect behavior similar to that observed with the scratch-wounded monolayer. Consistent with this prediction, we find that the epithelial sheet dynamics in the peel-off experiment qualitatively resembles the sheet dynamics in the scratch-wounding experiment. Specifically, there is a clear correlation between the displacements of cells and their location within the sheet (see Fig. 6*B*). The smaller overall displacements (Fig. 5*B*) can be attributed to the differences in the composition of the surfaces on which the cells are migrating. On the basis of these experiments, we conclude that mechanical injury provides the signals and stimuli necessary for the induction of the two waves of MAPK phosphorylation, and the coordination of cell dynamics necessary for epithelial cell sheet migration after wounding. We have confirmed that the MAPK phosphorylation patterns and sheet migration dynamics could be abolished by the addition of MAPK inhibitor (UO126), again in agreement with the results of Matsubayashi et al. (Figs. 5*D* and 6*D*).

Formation of ROS follows an injury and is responsible for initiating wound healing-like response. The well-organized spatiotemporal patterns of MAPK activation in wounded MDCK monolayers suggest an extensive degree of cell-cell communication. Among the numerous molecules that can mediate intercellular signaling are the extracellular calcium secreted growth factor and ROS. Furthermore, ROS have been shown to directly affect intracellular signaling, cytoskeletal dynamics, cell-cell adhesion, and cell motility (11, 20, 22, 23, 26). It is established that ROS, transiently generated under a variety of stress conditions, can couple to intracellular signaling pathways (24). We have hypothesized that ROS are involved in cell-cell coordination required for the generation of the traveling waves of MAPK activity. In one possible mechanism, ROS generated by a mechanical injury can be used as a fast way to propagate the information about the injury both within the cells and across the layer.

We used CM-H_2DCFDA as a reagent to visualize the spatiotemporal pattern of ROS distribution across the monolayer and found that, immediately after injury (on the time scale of seconds), a wave of ROS was formed. The ROS wave was

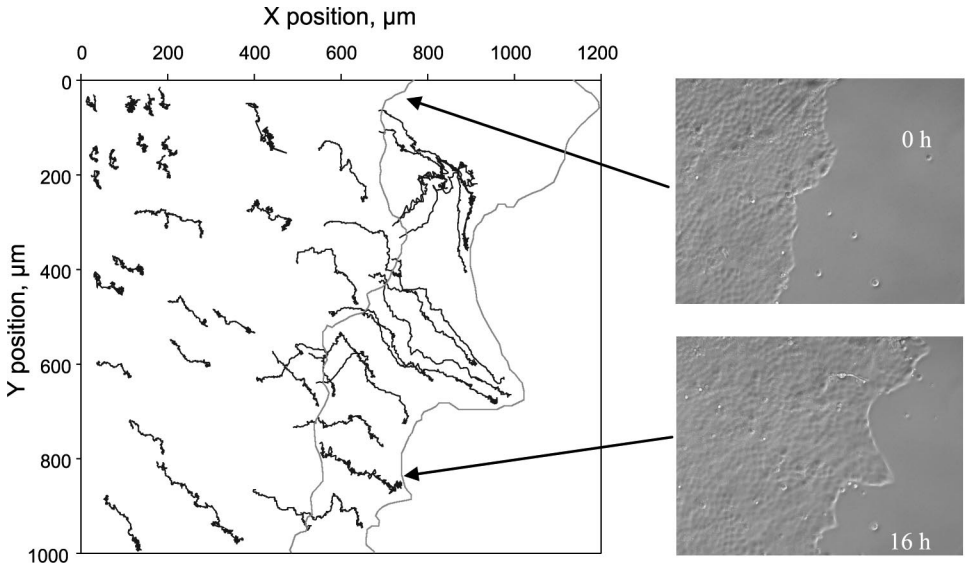

Fig. 4. Cell migration in an epithelial sheet wounded by scratching (45 randomly chosen cells were tracked for 16 h). *Right*, initial (0 h, *top*) and final (16 h, *bottom*) sheet images.

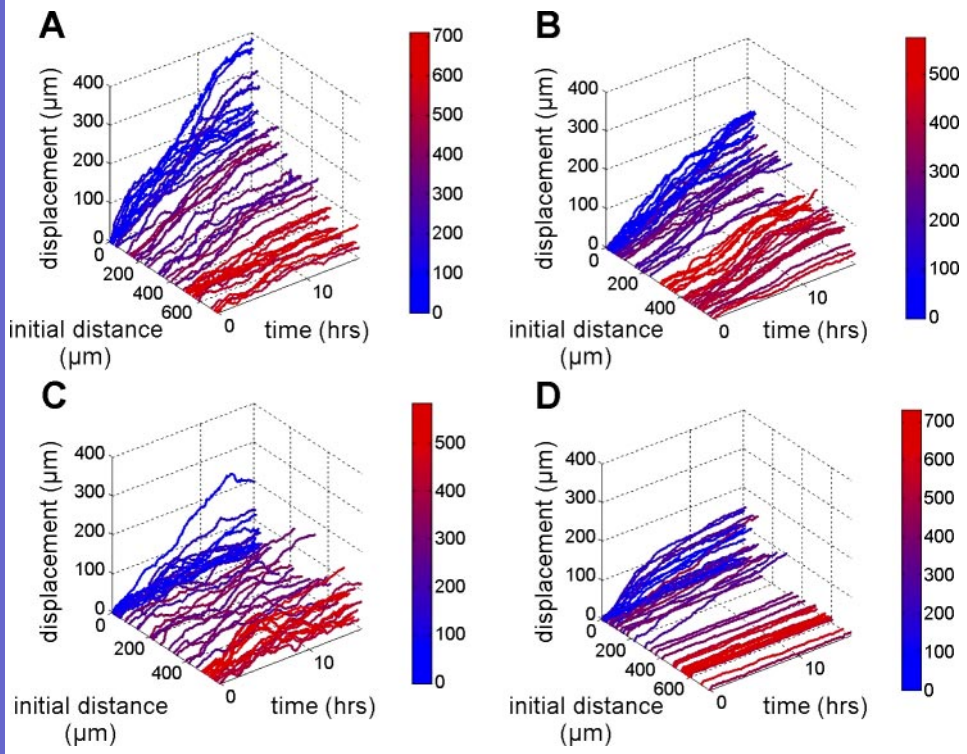

Fig. 5. Quantification of the sheet motion. For each of the four cases, temporal evolution of cells' displacement is shown with the color code referring to the initial position of a cell (micrometers from the wound interface). *A*: in the case of an injury by scratching, the closer the cell to the wound interface the greater is its displacement at all times during the sheet migration, as evidenced by the smooth transition of color from blue (close to the wound) to red (far away from the wound). *B*: in the case of an injury by membrane peel-off, a similar trend is observed with a decrease in the amplitude of displacements due to the difference in the surface on which the cells were migrating (see text for details). *C*: in the case of injury-free unconstraining, the initial position of a cell does not seem to be as important in determining the displacement of a cell as evidenced by the lack of a smooth transition of color from blue to red. *D*: inhibition of ERK1/2 MAPK prevents the transduction of the signal from the injury site to the rest of the sheet resulting in the motion of only the front cells and very little motion of the intermediate and back cells, as exhibited by minimal values of purple and red curves at all times during the cell sheet migration.

confined to the first few layers of cells immediately next to the wound interface and remained present for up to ~10 min after the injury (Fig. 8*A*).

If the formation of the ROS wave was abolished by an addition of the ROS inhibitor, *N*-acetyl-L-cysteine, the migration of the sheet was halted (Fig. 8*B*). This effect was similar to the one induced by the addition of the MAPK inhibitor; some cells at the wound interface exhibited some migratory behavior, whereas the rest of the sheet practically remained static. To further elucidate the connection between the formation of ROS and the activation of MAPK, we examined the pattern of ERK1/2 phosphorylation under conditions when the formation of ROS was inhibited. As expected, the pattern of MAPK activation was different with the distinct pattern of two waves of MAPK reaching deep into the sheet absent (Fig. 8*C*). Only the first few layers of cells next to the wound interface exhibited some MAPK activity. Taken together, these results suggest a direct connection between the immediate formation

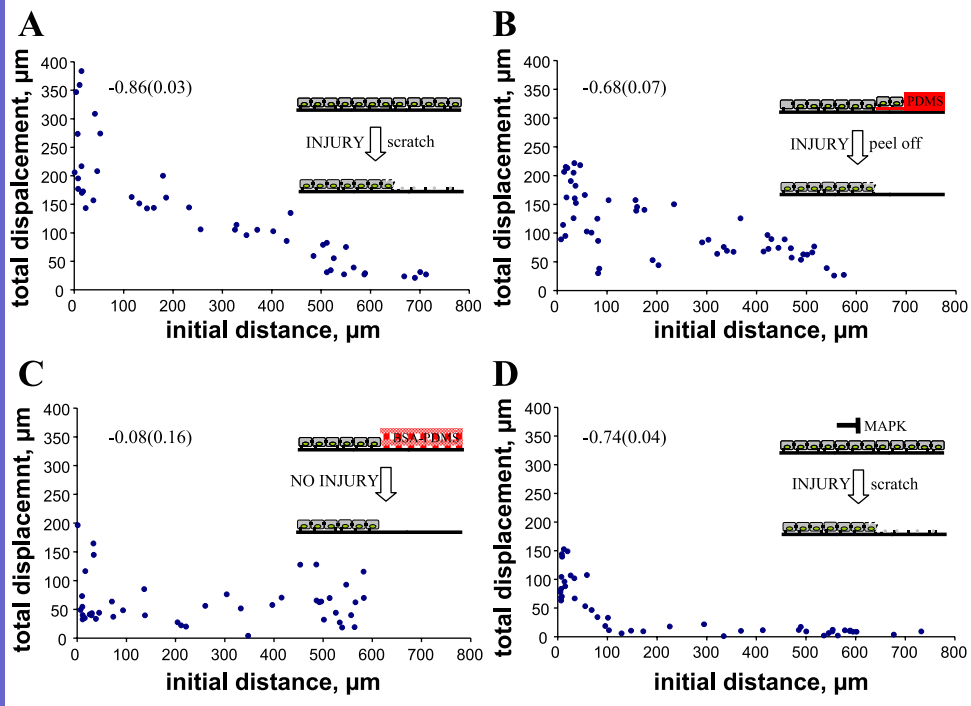

Fig. 6. Total displacement (TD) of individual cells as a function of distance from the wound. *A*: mechanical wounding by scratching. *B*: wounding by membrane peel-off. *C*: injury-free unconstraining. *D*: inhibition of ERK1/2 MAPK signaling. The correlation coefficient between TD and initial distance from wound is indicated on each graph along with the error.

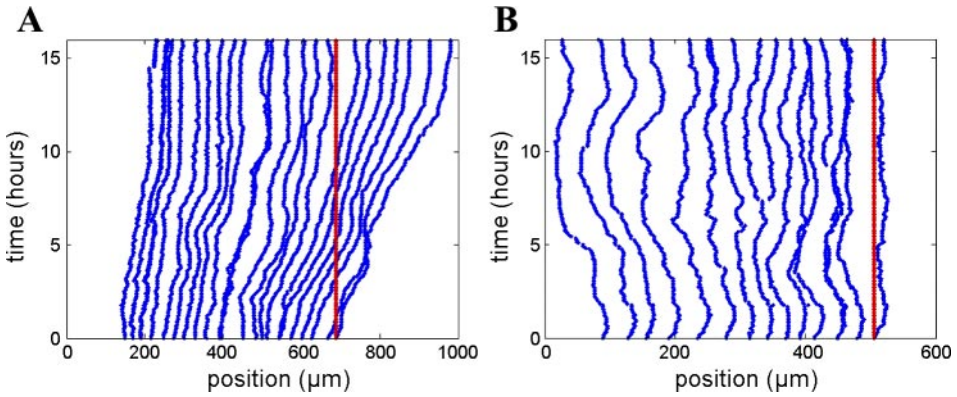

Fig. 7. Tracking of the line of cells perpendicular to the wound interface: distances of the individual cells from the interface followed as a function of time (the original position of the interface is marked by a line). *A*: in the case of wounding, a quasi one-dimensional motion is observed. *B*: in the case of unconstraining, no directed motion is observed.

of the ROS after an injury, which in turn leads to the activation of MAPK (Fig. 8*D*).

DISCUSSION

Our experimental approach allowed us to dissect the classical epithelial wound healing assay and to analyze how individual aspects of the wounding contribute to the coordinated dynamics of cells during epithelial sheet migration. We used three different conditions under which the cell sheet was observed: *1*) classic wound healing assay where a scratched monolayer migrates over the remnants of cell deposited extracellular matrix and other serum- and cell debris-adsorbed material, *2*) unconstraining with a slab of BSA-blocked PDMS, where an uninjured cell sheet migrates over plain tissue culture surface, and *3*) injury via PDMS membrane peel-off where an injured cell sheet migrates over plain tissue culture surface (Fig. 1*B*). Our main result is that, at least for MDCK epithelial sheets, injury provides a critical input required for cell-cell coordination in the spreading of the wounded monolayer. We also identified the presence of ROS in the first couple of cell layers next to the wound interface that are susceptible to mechanical damage. One of the ways in which the injury can directly lead to the onset of signaling within the sheet is through this formation of ROS, which we show leads to the activation of the MAPK signaling pathway.

Taken together, our signaling data and our tracking analysis suggest the following rudimentary sequence of events after an epithelial layer is mechanically injured: immediate formation of ROS, which then initiates the fast, transient ERK1/2 wave resulting in the initiation of the coordinated directed sheet

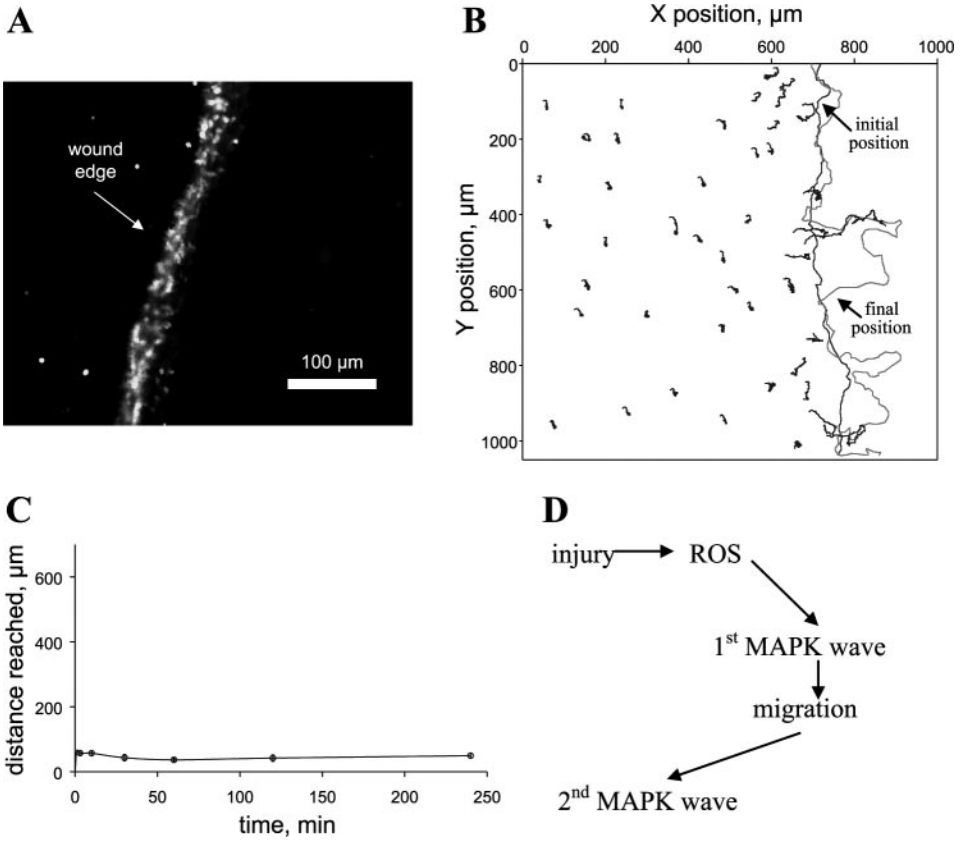

Fig. 8. *A*: immunofluorescent staining of reactive oxygen species (ROS). ROS formed immediately after injury and remained present in the first few rows of the epithelial sheet at the wound interface for ~10 min. *B*: migration of the sheet was halted when the ROS formation was inhibited pharmacologically: only some cells at the interface exhibited some migratory behavior, whereas the rest of the sheet remained static. *C*: waves of MAPK activation did not form when ROS formation was inhibited. *D*: possible sequence of events following an injury: immediate formation of ROS, followed by the first MAPK wave, which leads to migration that in turn leads to the second wave of MAPK activity.

migration. We can further speculate that it is the locomotion of individual cells in the sheet that leads to the activation of the slower wave of ERK1/2, consistent with the observation that the transient wave is present only in the case of an injury, whereas the slower, sustained wave is present in both the injury and the unconstrained case, both conditions under which cell locomotion is present (Fig. 8*D*).

The experimental system presented here allowed us to assess the relative contributions of the initial injury, MAPK signaling pathway, and the surface properties on the coordinated migration of an epithelial sheet. Our approach is well suited for further experimental studies of cell-cell coordination in the dynamics of epithelial sheets. Future work is required to investigate the biochemical and cellular origin of the waves of MAPK activation in wounded MDCK epithelial layers. While the original paper by Matsubayashi et al. proposed that these waves might be driven by local (mechanical) cell-cell interactions, several independent experiments point to several diffusible signals that might contribute to the observed spatiotemporal patterns of MAPK activation. Among these are extracellular Ca^{2+}, ATP, and peptide growth factors (5, 13, 14, 21a, 28). Furthermore, other signaling pathways, such as the JNK MAPK, are crucial for wound closure in the MDCK monolayers and several in vivo systems (1, 9). These signals can form a highly dynamic and spatially distributed network that regulates cell shape changes and cell-cell and cell-substrate interactions in spreading of the wounded epithelial sheet.

Experiments with MDCK epithelial sheets and our methods for systematic manipulation of initial and boundary conditions are ideally suited for the analysis of emerging collective behavior in wounded epithelial layers. When coupled with the analysis of mechanical behavior of cells (their morphology and forces exerted on the substrate and one another) and cell-cell signaling these studies can lead to the formulation of mechanistic descriptions of coordinated cell dynamics in epithelial layers (8, 18, 21b). The advanced models for migration of individual cells can form the starting point for these models (6, 7, 10).

ACKNOWLEDGMENTS

The authors are indebted to Jean Schwarzbauer for helpful discussions and suggestions during the course of this project. D. L. Nikolic, A. N. Boettinger, and S. Y. Shvartsman thank Toly Rinberg for help with cell tracking and Ron Weiss for lending a live stage microscope for use in this study.

GRANTS

This work was supported by the grants from National Science Foundation and National Institutes of Health (to S. Y. Shvartsman), and by the Merck Summer Undergraduate Research Fund program (to A. N. Boettinger).

REFERENCES

1. **Altan ZM and Fenteany G.** c-Jun N-terminal kinase regulates lamellipodial protrusion and cell sheet migration during epithelial wound closure by a gene expression-independent mechanism. *Biochem Biophys Res Commun* 322: 56–67, 2004.
2. **Block ER, Matela AR, SundarRaj N, Iszkula ER, and Klarlund JK.** Wounding induces motility in sheets of corneal epithelial cells through loss of spatial constraints. Role of heparin-binding epidermal growth factor-like growth factor signaling. *J Biol Chem* 279: 24307–24312, 2004.
3. **Brodu V, Elstob PR, and Gould AP.** EGF receptor signaling regulates pulses of cell delamination from the *Drosophila* ectoderm. *Devel Cell* 7: 885–895, 2004.
4. **Chen Z, Gibson TB, Robinson F, Silvestro L, Pearson G, Xu BE, Wright A, Vanderbilt C, and Cobb MH.** MAP kinases. *Chem Rev* 101: 2449–2476, 2001.
5. **Chung E, Graves-Deal R, Franklin JL, and Coffey RJ.** Differential effects of amphiregulin and TGF-α on the morphology of MDCK cells. *Exp Cell Res* 309: 149–160, 2005.
6. **Dallon JC and Othmer HG.** How cellular movement determines the collective force generated by the *Dictyostelium discoideum* slug. *J Theor Biol* 231: 203–222, 2004.
7. **Dimilla PA, Barbee K, and Lauffenburger DA.** Mathematical model for the effects of adhesion and mechanics on cell-migration speed. *Biophys J* 60: 15–37, 1991.
8. **Du Roure O, Saez A, Buguin A, Austin RH, Chavrier P, Siberzan P, and Ladoux B.** Force mapping in epithelial cell migration. *Proc Natl Acad Sci USA* 102: 2390–2395, 2005.
9. **Galko MJ and Krasnow MA.** Cellular and genetic analysis of wound healing in *Drosophila* larvae. *Plos Biol* 2: 1114–1126, 2004.
10. **Gracheva ME and Othmer HG.** A continuum model of motility in ameboid cells. *Bull Math Biol* 66: 167–193, 2004.
11. **Gregg D, Rauscher FM, and Goldschmidt-Clermont PJ.** Rac regulates cardiovascular superoxide through diverse molecular interactions: more than a binary GTP switch. *Am J Physiol Cell Physiol* 285: C723–C734, 2003.
12. **Kane RS, Takayama S, Ostuni E, Ingber DE, and Whitesides GM.** Patterning proteins and cells using soft lithography. *Biomaterials* 20: 2363–2376, 1999.
13. **Kimura K, Nishimura T, and Satoh Y.** Effects of ATP and its analogues on $Ca^{2+}{}_i$ dynamics in the rabbit corneal epithelium. *Arch Histol Cytol* 62: 129–138, 1999.
14. **Klepeis VE, Weinger I, Kaczmarek E, and Trinkaus-Randal V.** P2Y receptors play a critical role in epithelial cell communication and migration. *J Cell Biochem* 93: 1115–1133, 2004.
15. **Lauffenburger DA and Horwitz AF.** Cell migration: a physically integrated molecular process. *Cell* 84: 359–369, 1996.
16. **Martin P and Parkhurst SM.** Parallels between tissue repair and embryo morphogenesis. *Development* 131: 3021–3034, 2004.
17. **Martinez-Arias A and Stewart A.** *Molecular Principles of Animal Development*. New York: Oxford University Press, 2002.
18. **Matsubayashi Y, Ebisuya M, Honjoh S, and Nishida E.** ERK activation propagates in epithelial cell sheets and regulates their migration during wound healing. *Curr Biol* 14: 731–735, 2004.
19. **Mine N, Iwamoto R, and Mekada E.** HB-EGF promotes epithelial cell migration in eyelid development. *Development* 132: 4317–4326, 2005.
20. **Nimnual AS, Taylor LJ, and Bar-Sagi D.** Redox-dependent downregulation of Rho by Rac. *Nat Cell Biol* 159: 361–370, 2003.
21. **Ostuni E, Kane R, Chen CS, Ingber DE, and Whitesides GM.** Patterning mammalian cells using elastomeric membranes. *Langmuir* 16: 7811–7819, 2000.
21a. **Pribyl M, Muratov CB, and Shavartsman SY.** Long-range signal transmission in autocrine relays. *Biophys J* 84: 883–896, 2003.
21b. **Pribyl M, Muratov CB, and Shvartsman SY.** Discrete models of autocrine cell communication in epithelial layers. *Biophys J* 84: 3624–3635, 2003.
22. **Storz P.** Reactive oxygen species in tumor progression. *Front Biosci* 10: 1881–1896, 2005.
23. **Taniyama Y and Griendling KK.** Reactive oxygen species in the vasculature: molecular and cellular mechanisms. *Hypertension* 42: 1075–1081, 2003.
24. **Torres M.** Mitogen-activated protein kinase pathways in redox signaling. *Front Biosci* 8: D369-D391, 2003.
25. **Wasserman L.** *All of Statistics: A Concise Course in Statistical Inference*. New York: Springer, 2003.
26. **Wu RF, Xu YC, Ma Z, Nwariaku FEA, Sarosi GA, and Terada LS.** Subcellular targeting of oxidants during endothelial cell migration. *J Cell Biol* 171: 893–904, 2005.
27. **Xia Y and Kao WW.** The signaling pathways in tissue morphogenesis: a lesson from mice with eye-open at birth phenotype. *Biochem Pharmacol* 68: 997–1001, 2004.
28. **Xu KP, Ding Y, Ling J, Dong Z, and Yu FS.** Wound-induced HB-EGF ectodomain shedding and EGFR activation in corneal epithelial cells. *Invest Ophthalmol Vis Sci* 45: 813–820, 2004.
29. **Zhang Z, Oliver P, Lancaster SR, Schwarzenberger PO, Joshi MS, Cork J, and Kolls JK.** Reactive oxygen species mediate tumor necrosis factor alpha-converting, enzyme-dependent ectodomain shedding induced by phorbol myristate acetate. *FASEB J* 15: 303–305, 2001.